DOI: https://doi.org/10.24425/amm.2025.154488

O.V. IVANOVA^{1,2*}, V.V. SAVINKIN^{1,2*}, A.K. TULESHOV¹, A.V. SANDU^{3,4,5,6}, P. VIZUREANU^{3,7*}

THE EFFECT OF VIBRATION FREQUENCY ON THE PHYSICAL AND MECHANICAL PROPERTIES OF THE MATERIAL AND THE PHASE STRUCTURE OF THE PUMP PART

The article solves the scientific and technical problem of studying the effect of vibration loads on the phase structure of the material and the durability of a centrifugal pump. It was found that the natural frequencies of the impeller (>100 Hz) are 75% higher than the operating speed of the structure (25 Hz), which indicates sufficient rigidity of the wheel structure for the selected materials 12Cr7Mn3SiC. The scientific novelty is represented by the established dependences of changes in the frequency range of vibrations leading to the formation of stresses, a decrease in the physico-mechanical properties of the phase structure of the material from dynamic loads of different forms of vibrations. The optimal range of permissible frequency oscillations of the system and the object that are not in the resonant state is justified. The theoretical significance is reflected in the systematization of structural and frequency-vibration factors affecting the formation of fatigue stress concentrations and the origin of microcracks in the phase structure of perlite. At a distance of 3 mm from the crack, a transition to a more dispersed structure is established, the characteristic size of ferritic grains decreases to 5-10 μ m. It was found that at a distance of less than 100 μ m from the crack, the hardness increases (~240 HV for ferrite and ~260 HV for perlite). Thus, cyclic loads of vibrational frequencies led to grain grinding, an increase in hardness and the appearance of a crack in the most loaded part of some samples. The acquired knowledge allows us to predict defects with high accuracy at the stage of pre-destruction of the molecular bonds of the material structure.

Keywords: Vibration frequencies; phase structure; centrifugal pump; modeling; physical and mechanical properties; durability

1. Introduction

The resource durability of parts of dynamic aggregates forming technical systems operating under load depends on many well-known factors. For well-known reasons, when developing measures to increase the durability of a part, the loads acting on contact or mating surfaces operating in an aggressive environment of interaction are primarily considered. Having determined the load mode and the interaction medium, the brand of the material, its physical and mechanical properties and the phase structure of the transition zones to the base of the material are selected.

Parts of mechanisms and machines are subjected to significant mechanical influences during operation – vibration, shock and linear loads. The resulting loads cause mechanical stresses in individual parts of dynamic units and form zones of fatigue

stress concentration. This can lead to disruption of the normal operation of the entire system or its failure. Vibrations occurring in a certain range of natural frequencies lead to internal degradation of the structure of the material of the component structure, which can lead to its further destruction [1,2].

When performing design calculations, having determined the loading modes and the interaction medium, they are determined with the choice of the material brand, its physicomechanical properties and the phase structure of the transition zones to the base of the material. But the question remains open about the influence of the physico-mechanical characteristics of the material used to manufacture parts under the influence of dynamic loads on the magnitude and shape of the natural vibrations of the structure. The question also arises about the possibility of determining the optimal phase structure of the material that is resistant to resonant vibration modes of the system, establishing

^{*} Corresponding authors: cavinkin7@mail.ru, itf.nkzu@mail.ru, sav@tuiasi.ro



JOLDASBEKOV INSTITUTE OF MECHANICS AND ENGINEERING; 28, SHEVCHENKO STR., ALMATY, 050010, KAZAKHSTAN

M. KOZYBAEV NORTH KAZAKHSTAN UNIVERSITY, TRANSPORT AND MECHANICAL ENGINEERING DEPARTMENT, 86, PUSHKIN STREET., PETROPAVLOVSK, 150000, KAZAKHSTAN

³ GHEORGHE ASACHI TECHNICAL UNIVERSITY OF IAŞI, FACULTY OF MATERIALS SCIENCE AND ENGINEERING, BOULEVARD D. MANGERON, NO. 51, 700050 IASI, ROMANIA
4 ROMANIAN INVENTORS FORUM STR. P. MOVII & 3, 700089 IASI, ROMANIA

⁴ ROMANIAN INVENTORS FORUM, STR. P. MOVILA 3, 700089 IASI, ROMANIA
5 NATIONAL INSTITUTE FOR RESEARCH AND DEVELOPMENT FOR ENVIRONMENTAL PROTECTION INCOPM, 294 SPLAIUL INDEPENDENTEI, 060031 BUCHAREST, ROMANIA

ACADEMY OF ROMANIAN SCIENTISTS, 54 SPLAIUL INDEPENDENTEI ST., SECT. 5, 050094 BUCHAREST, ROMANIA;

TECHNICAL SCIENCES ACADEMY OF ROMANIA, DACIA BLVD 26, 030167 BUCHAREST, ROMANIA

the causes of crack formation from a certain range of resonant frequencies of vibrations in real operating conditions.

During operation, centrifugal pumping units often experience a special hydrodynamic regime, accompanied by vibration of all parts of the structure. Increased vibration exposure leads to an intensive process of wear and destruction of pump parts, that is, the consequences of vibration can become not only negative, but also dangerous. The impeller is one of the main elements of a centrifugal pump, which has high requirements for reliability and durability. In this regard, the problem of reducing the vibration effect on the impeller of a centrifugal pump is one of the priorities in increasing the service life of the entire pump as a whole.

Therefore, there is a scientific and technical task, which is as follows: in order to obtain the optimal combination of properties and structural components of a structural material (grain size, phase composition – fine-grained martensite) to ensure the calculated operational parameters of parts and assemblies of machines that perceive vibration loads, it is necessary to conduct a study of the effect of cyclically varying operating load and manufacturing technology of parts on the physical and chemical properties ofmechanical properties of the construction material during long-term operation of the pump.

In the production environment, the required properties are formed by technological methods of exposure. For the objectivity and reliability of the research results and the establishment of uniform conditions for the propagation of frequency vibrations, let us consider two different dynamic systems. The first system is the "Impeller – Shaft of a centrifugal pump" and the second is the "Wheel of a railway carriage – Rail", operating in radically different environments.

For example, 20Cr13C and 12Cr7Mn3SiC steels with the following material characteristics are used to manufacture the impeller of a centrifugal oil pump (Fig. 1):

yield strength is 450 [N/mm²] and 1,079 [N/mm²], respectively;

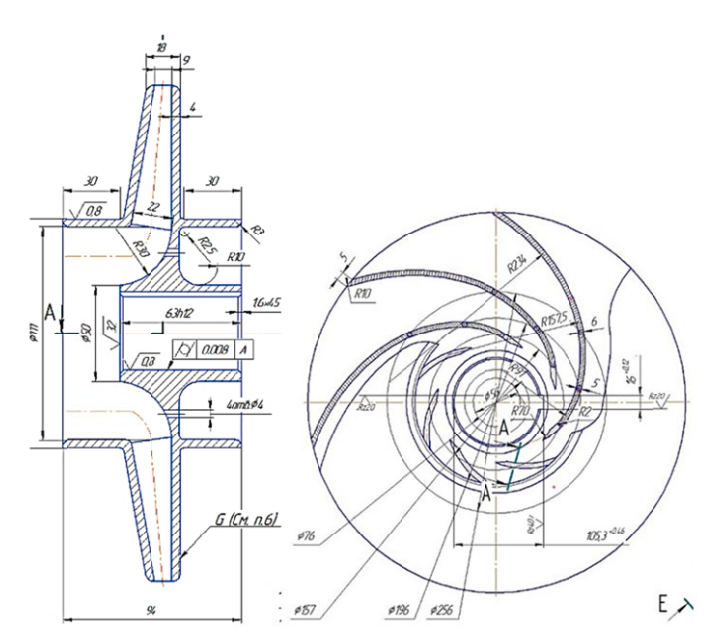


Fig. 1. Impeller of a centrifugal pump

- the normal modulus of elasticity is 222,000 [N/mm²] and 210,000 [N/mm²], respectively;
- the temperature coefficient of linear expansion is 0.00001 [1/C°] and 0.000012 [1/C°], respectively;
- the compressive strength is 200 [N/mm²] and 1,324 [N/mm²], respectively;
- the tensile strength limit is 210 [N/mm²] and 553 [N/mm²], respectively;
- the torsional endurance limit is 150 [N/mm²] and 331 [N/mm²], respectively.

2. Materials and methods

In the manufacture of wheelsets (Fig. 2) of railway wagons, foundry alloys of Steel of groups 1, 2, 3, 4 are also used. Medium carbon steels with a carbon content of 0.3...0.6%. These steels have σ_b from 400 to 800 MPa, d from 20 to 25% and HB from 1,400 to 2,000 MPa. They are used as engineering steels for the manufacture of machine parts. As a rule, they are subjected to hardening heat treatment.

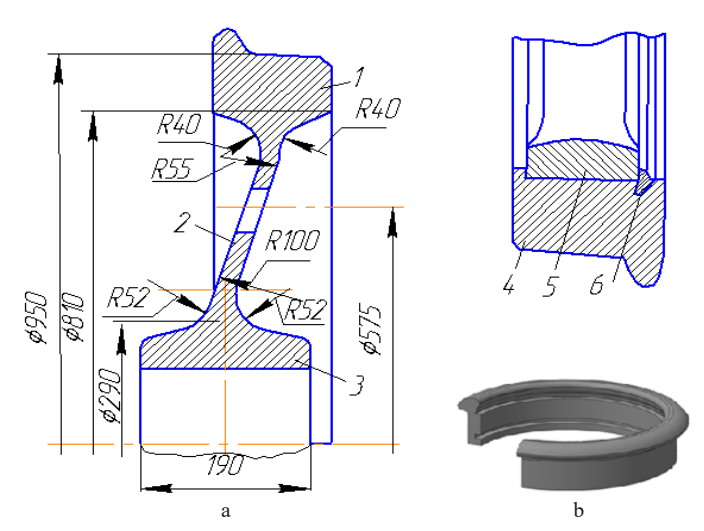


Fig. 2. Profile of a standard wagon wheel: a – bandless solid-rolled; b – bandage: 1 – rim; 2 – disc; 3 – hub; 4 – bandage; 5 – wheel center; 6 – reinforcing ring

As noted, these types of grades (20Cr13C, 12Cr7Mn3SiC, Steel 1 and Steel 2) of the material are widely used in many branches of mechanical engineering and the oil and gas industry (impeller of a centrifugal pump and wheel pairs of railway wagons). The life cycle of the durability of these parts is determined by the ability of their material to resist the negative effects of external dynamic forces and their moments. Each type of material has a safety factor, which depends on the mechanical properties of the metal. Inevitably, during operation, the contact surfaces are subject to degradation and this is determined visually, by measuring and calibration tools almost at the last stage of the part's life cycle. However, in the practice of operation, sudden failures, breaks and warping of metal occur at first glance with an ideal surface, without visible defects. This phenomenon occurs during

Optimal steel parameters of railway carriage wheels after thermal exposure to highly concentrated energy sources

The brand of the metal of the wheelset	Elongation, not less than	Relative narrowing, not less than	Surface hardness, HB	Ultimate strength, MPa	Brittleness at 20°C, MJ/m ²
Steel 1	12%	21%	248	880-1,080	0,3
Steel 2	8%	14%	255	912-1,107	0,2

the formation of critical conditions of the metal yield strength and the rupture of interatomic bonds in the metal structure. Scientists Ivanova O.V., Savinkin V.V., Shvindin A.I. [2-4] proved that the concentration of internal fatigue stresses plays an essential role in the formation of a defect. The magnitude of fatigue stresses, their location zones and the formation time in the phase structure of each material are different (20Cr13C, 12Cr7Mn3SiC, Steel 1 and Steel 2). Also, these grades of material with high physical and mechanical properties have different durability resources. The problem is that the impeller of the centrifugal pump experiences minor dynamic loads, but is subject to intense vibration vibrations. It is the range of oscillation frequencies that leads to internal degradation of the structure and its destruction, although external loads are insignificant.

Therefore, it is hypothesized that the study of the process of changing the phase structure of a metal under the influence of dynamic loads and natural vibration frequencies will allow predicting the service life and the zone of defect formation at the stage of its origin.

Vibration of machines and mechanisms in general is a complex process that is mathematically difficult to describe. The harmful effects of vibration of machines are expressed in a decrease in their reliability and durability, unplanned repairs, the creation of emergency situations, and violation of the technological regime. The reliability of centrifugal pumps, as a type of dynamic machines, is determined to a large extent by their vibration reliability. A low and stable vibration level, the absence of resonant and self-oscillating phenomena in the entire range of operating modes guarantees the required reliability and durability. According to statistics, due to increased vibration, more than 60% of failures of centrifugal pumps in oil refining occur. What are the main sources of vibration and how can negative consequences be avoided? The issue has not been resolved [2,3,5].

From the analysis of the causes of defects, additional parameters have been established that are not taken into account when designing the impeller and the pump impeller, such as: the concentration of internal stresses in the structure of the martensitic metal; the difference in electrode potentials of two or more materials acting as an anode and cathode; the natural oscillation frequency and amplitude of the system; the balancing temperature coefficient of expansion of the shaft and impeller material.

The most common criteria for pump quality are the following values:

- pump life;
- weight and size parameters of the pump;
- the pump efficiency;
- dynamic characteristics.

Creating a methodology for calculating optimal pump parameters that can satisfy all these criteria at the same time is a difficult task. The study of the characteristics of free vibrations is an important and science-intensive process, since it is the natural frequencies and their corresponding eigenforms that completely determine the individual physical and dynamic properties of a mechanical system and help in the analysis of forced vibrations [5,6].

The harmful effects of vibration of machines are expressed in a decrease in their reliability and durability, unplanned repairs, the creation of emergency situations, violation of the technological mode of operation. The described processes are caused by the degradation of the metal structure, by the destruction of interatomic bonds by low-frequency vibrations. The destruction of interatomic bonds entails a change in the structural grains and modification of phase transformations with the focus of fatigue stresses, which concentrate microcracks in the parts and, accordingly, reduce the mechanical properties of the material.

Studies have shown a significant influence of the geometric dimensions and shapes of parts, as well as the influence of material properties on the vibration characteristics of parts and their ability to increase vibration resistance. Investigating the hydrodynamics of a centrifugal pump, with the specified kinematic characteristics of the parts, the authors paid attention to the following types of vibrations: mechanical nature; hydrodynamic; cavitation.

The reason for the mechanical nature of the occurrence of vibrations is the dynamic imbalance of the impellers and the pump shaft. That is, an imbalance under the influence of the moment of inertia forms variable loads on the rotor supports and bending of the shaft (Fig. 3).

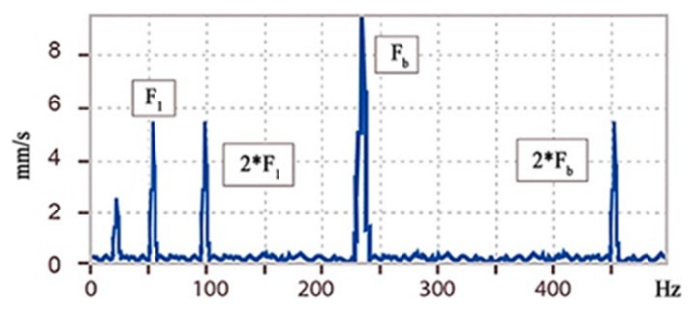


Fig. 3. Vibration spectrum of the pump with increased blade vibrations: F_1 – rotor speed; F_b – blade frequency

During this period, the risks of dangerous resonant vibrations are formed, in which significant axial movements occur in the mechanisms caused by the coincidence of harmonic loads with natural frequencies (Fig. 3) [4,5,7-9].

The unsteadiness of the flow in the flow part of the pump forms the hydrodynamic character of vibrations, which causes pulsations of velocities and pressures and, consequently, pulsating radial force. In particular, the separation of the boundary layer from the profiles of the paddle wheel in under-loading (with supplies of less than optimal) modes causes recirculation of the flow in its channels, which contributes to the formation of rotating and constantly changing vortex zones at the entrance to the paddle wheel. The presence of vortex zones causes powerful pulsation phenomena in the entire flow part of the pump and increased vibrations of the bearing supports (Fig. 4) [4,5,7-9].

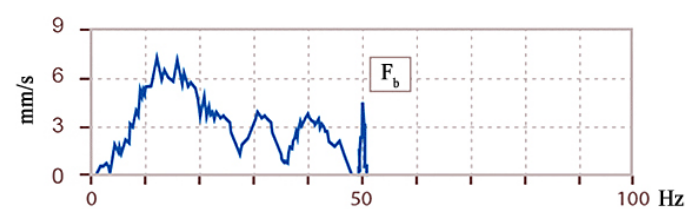


Fig. 4. Vibration spectrum of a pump with flow turbulence: F_b – blade frequency

A powerful source of random vibration is cavitation, which also occurs when the blades flow around (Fig. 5). Cavitation collapse of gas bubbles, mainly on the blades of the impeller, is a very harmful phenomenon that destroys the working surface of the blades. The power of this component of random vibration is also modulated by the rotational frequency of the impeller, the blade frequency or the frequency of self-oscillation of the rotor [4,5,7-9].

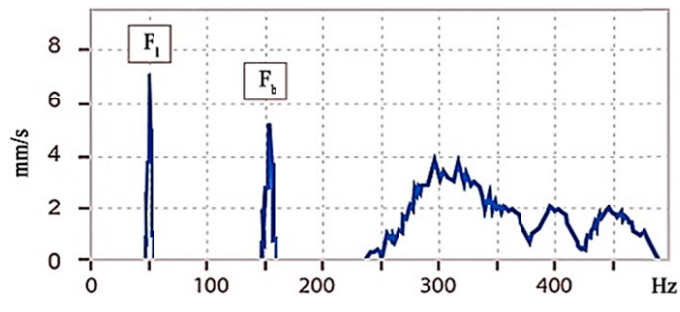


Fig. 5. Vibration spectrum of the pump with cavitation effect: F_1 – rotor speed; F_b – blade frequency

An important component is the dynamic calculation, since the voltages of σ_d are many times higher than static σ_{st} . The operation of the pump is accompanied by cyclically unstable loading of its structure, as a result of which vibration occurs. Therefore, when designing a pump, it is a mandatory requirement not only to study the elements of its structure for strength and rigidity, but also to conduct special studies related to determining the dynamic characteristics of the impeller blades and directly critical frequencies [8,10,11].

When designing a centrifugal pump, it is important to understand the dependence of critical and maximum permissible operating conditions on resonant frequencies. By studying the characteristics of free frequencies and their corresponding eigenforms, the individual dynamic properties of the mechanical system, the physico-mechanical properties of the material and the phase structure are determined, which are crucial in the analysis and evaluation of the critical values of forced oscillations [12].

The mean square deviation value of vibration acceleration a(t), vibration velocity v(t) and vibration displacement S(t) were used as a model of the vibration level of the unit [13,14]. For a pump, the RMS value of any of these three vibration values characterizes the vibration energy. It is established that the mean square deviation value of the vibration parameter is directly proportional to the destructive vibration force of the pump. Accordingly, by increasing the mean square deviation value of vibration, it is possible to predict and prevent pump failure. The study of dynamic and hydrodynamic processes was carried out using computer modeling of CAD/CAM systems.

The purpose of the study is to study the influence of the physico-mechanical characteristics of the material used to manufacture the impeller of a centrifugal pump on the magnitude of the natural frequency and shape of the oscillations of the impeller under the influence of dynamic loads. The scientific problem lies in the absence of a single method for determining the optimal phase structure of a material that is resistant to resonant vibration modes of pump operation and establishing a causal relationship between crack generation from low resonant vibration frequencies in real operating conditions.

To assess the stress-strain state of the impeller of a single-stage, cantilever, centrifugal pump type centrifugal horizontal pump (CHP 150-315) (pump brand), its finite element model has been developed. The geometric model of the blade was developed in the CFturbo software package (Fig. 6). Further, based on the obtained blade profile, a simulation of the pump impeller was performed in the Compass-3D software environment (Fig. 6).



Fig. 6. 3D model of the blades and impeller of the pump, made in the CFturbo software environment

The finite element model is built in the software package of the strength analysis system designed to work in the interface (APM FEM) strength analysis system on 4-node tetrahedra, containing 64,552 nodes and 227,600 finite elements.

The statistical range of operating pressures (*P*) from 1.5 to 4 MPa is selected for calculations. The APM FEM software package performs Linear static calculation, Stability calculation and Natural frequency calculation taking into account preloading for various grades of structural materials.

The results of modeling the loads on the working surfaces of the pump impeller are:

- distribution of equivalent stresses and their components, as well as the main stresses;
 - distribution of linear, angular and total displacements;
- distribution of deformations by model elements;
- distribution of reserve coefficients by yield strength and strength;
- coordinates of the center of mass, mass, moments of inertia of the model;
- total reactions reduced to the center of mass of the model.

In the study of the strength characteristics of the working elements, the criterion for the durability of the pump is the voltage σ . The equivalent stresses (σ_e) according to the fourth theory of the strength of the pump structure during dynamic calculation were determined for materials 20Cr13C and 12Cr7Mn3SiC at a pressure of P = 1.5; 2.5 and 4 MPa (1) [15-17]:

$$\sigma_e = \sqrt{\left(\sigma_b + \sigma_{str}\right)^2 + r\tau^2} \le [\sigma] \text{ or } \sigma_d = \sigma_{st} \cdot K_d \qquad (1)$$

where σ_b – the bending stress; σ_{str} – the tensile stress; τ – the torsional stress; σ_d – the stress during dynamic calculation; σ_{st} – the stress during static calculation; K_d – the coefficient of dynamism.

Steel 20Cr13C is used for the manufacture of castings of parts subjected to shock loads (turbine blades, etc.), products

TABLE 2 Mises voltages in the pump impeller (n = 1,500 rpm)

Pressure, MPa	Equivalent Mises voltage, σ_{\min} and σ_{\max} (MPa) (Material)					
MIFA	Steel 20Cr13C	Steel 12Cr7Mn3SiC				
1.5	MATIM 108 108 109 109 109 109 109 109	TATM 107 108 108 108 108 108 108 108				
4.0	700 100 100 100 100 100 100 100 100 100	761 ATEM 301 306 306 306 307 308 308 308 308 308 308 308				

TABLE 3 Complete deformation of the impeller (n = 1,500 rpm)

Pressure,	Total linear displacement, mm (Material)					
MPa	Steel 20Cr13C	Steel 12Cr7Mn3SiC				
1.5	**************************************	### APPM # 657 # 620 1 768 4 80				
4.0	MATM TO 1 TO 2 TO 1 TO 2 TO 3 TO 4 TO 3 TO 3 TO 3 TO 4 TO 4	75 ATM 25 55 26 5 26 6 20 6 20 6 20 6 20 7 20 6 20 6 20 7 20 7 20 7 20 7 20 7 20 7 20 7 20 7				

exposed to weak aggressive media; castings of parts of gas turbines and axial compressors and others. Steel 12Cr7Mn3SiC is used for the manufacture of critical high-load parts operating under static and dynamic loads.

The results of calculations of the yield strength reserve coefficient and the tensile strength reserve coefficient are presented in TABLES 4 and 5.

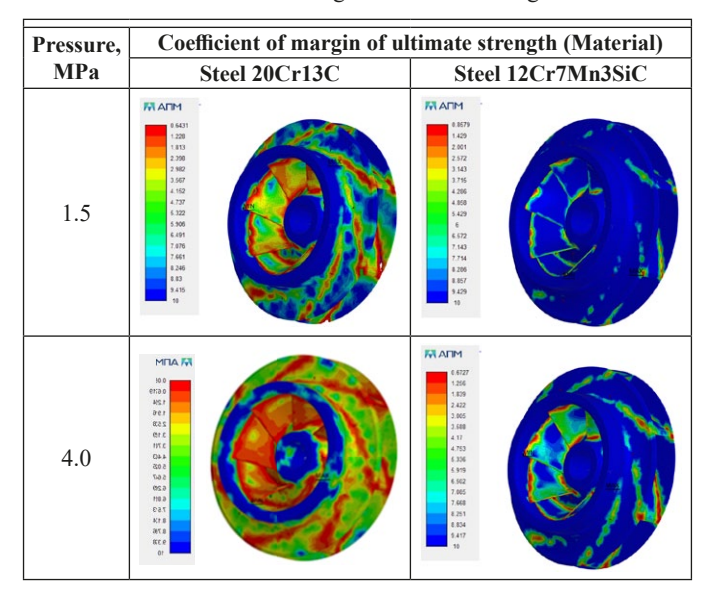
TABLE 4
Yield strength margin ratio

Pressure,	ssure, Yield strength margin ratio (Mater				
MPa	Steel 20Cr13C	Steel 12Cr7Mn3SiC			
1.5	0667 1020 1020 1020 1020 3030 430 430 430 430 430 430 430 430 4	# 1542 1 (20) 1 (20) 2 (20) 2 (20) 2 (20) 2 (20) 4 (20) 4 (20) 4 (20) 4 (20) 4 (20) 4 (20) 4 (20) 4 (20) 4 (20) 5 (20) 6 (20) 6 (20) 6 (20) 7 (20) 8 (20)			
4.0	61 0788 1330 1330 1330 1330 1330 1330 1330 13	# 5500 1027 1037 1031 1031 1031 1031 1031 1031 103			

A preliminary assessment of the simulation of the stress-strain state of the impeller showed that the greatest stress concentration is observed at the interface of the blades and the impeller covers. This problem is solved by constructive measures – the introduction of fillets and chamfers at the junction of the mating surfaces, which were not taken into account in the calculation model to simplify and reduce the calculation time. Steel 12Cr7Mn3SiC with the lowest modulus of elasticity

Coefficient of margin of ultimate strength

TABLE 5



 $(E = 2.1 \cdot 10^5 \text{ MPa})$ has a higher yield strength $[\sigma_s] = 1,079 \text{ MPa}$, which makes it possible to perceive large loads. That is, when designing parts exposed to dynamic loads, it is necessary to take a more careful approach to the choice of material and the ratio of its main determining parameters – yield strength (σ_s) , modulus of elasticity (E) and Poisson's ratio (μ) .

Dynamic frequency studies are due to the fact that in the case of coincidence of the external periodic load with the natural frequencies of the system (Impeller – Shaft), a resonance phenomenon occurs, which causes vibration, a multiple increase in stresses, which leads to the destruction of the entire pump structure.

The frequencies of free oscillations of the system are closely related to the corresponding eigenforms. The shapes and frequencies of vibrations are integral parameters of the system. They must be determined at the design stage of the structure in order to avoid destruction during testing. In the case of the impeller, analytical formulas give an approximate result; the finite element method (FEM) gives a more accurate result. The FEM also allows you to take into account the change in the stiffness of the impeller from the action of centrifugal forces.

It is well known that resonances are observed at frequencies close to the frequencies of natural vibrations of the structure. However, the issue of changes in the phase structure of the martensitic class of steels under the influence of vibrational vibrations at the stage of the beginning of the destruction of interatomic bonds, leading to pores and microcracks, has not been studied. Checking the spectral properties of the structure for the possibility of resonances in the operating frequency range of external influences at the design stage allows you to make changes to the design that can change the spectrum of natural frequencies. This will avoid or significantly reduce the likelihood of resonances, failures and increase the service life of pumps during operation.

The vibration intensity of the component parts of the equipment is generally expressed as a function $V = \varphi(F, n, \delta, C)$, where

F – the vibration–stimulating forces; η – the degree of detuning of the oscillating system from resonances; δ – the damping characteristic of the system; C – the stiffness characteristic of the system [13,18].

The main factor determining the vibration parameters of the equipment is the exciting forces. The other three factors form a group of conditions that determine the intensity of the manifestation of exciting vibration forces, that is, $y = \psi(\eta, \delta, C)$, where y – the condition for the manifestation of exciting vibration forces. Then the vibration intensity will have the following form $V = \varphi(F, y)$.

Numerically, the equation of motion of the pump rotor, taking into account oscillatory processes, is expressed as [19-22]:

$$[M]{a} + [H]{v} + [K]{S} = {P(t)}$$
 (2)

where [M] – the mass matrix of the mechanical system; [H] – the dissipation matrix of the mechanical system; [K] – the stiffness matrix of the mechanical system; $P(t) - \{a\}, \{v\}, \{S\}$ – the movements of the nodes and their first and second time derivatives.

The nature of natural oscillations is determined mainly by the system's own parameters: mass, elasticity, and others. Usually, natural vibrations fade over time, due to the influence of resistance forces (friction) in the system. Therefore, to determine the natural oscillation frequencies, consider free undamped oscillations, that is, H = 0 and P(t) = 0.

In this case, the oscillation of all points of the system occurs according to a sinusoidal law:

$$q = A_0 \sin(\omega t + \varepsilon) \tag{3}$$

$$S = S(t) = S_0 \sin(\omega_0 t + \varphi) \tag{4}$$

where ω_0 – the natural frequency; A_0 – the shape of the oscillation

Thus, the equation of motion of the centrifugal pump shaft has the following form:

$$(K - \omega^2 \cdot M) \cdot A = 0 \tag{5}$$

To obtain more accurate values of the free vibrations of the rotor, it is necessary to take into account the elastically malleable properties of the rolling bearings and the attached mass of liquid constantly concentrating in the flow part of the pump.

The stiffness coefficient of the supports k is determined by the ratio [19,20]:

$$k = \frac{R}{\varepsilon} \tag{6}$$

where R – the resulting reaction force of the support, N; ε – the deformation of the support, under the action of dynamic loads, m.

Knowing the elastic properties of the supports and the attached mass of the liquid, we determine the proper vibrations of the pump rotor.

The equation of forced vibrations of the rotor is described by the expression (1), where the centrifugal force of inertia F_i and is taken as the forced force. In matrix form, the general

equation of undamped forced rotor vibrations has the following form [20,23]:

$$[M]{a} + [H]{v} + [K]{S} = F_u = [M \cdot e]\omega_0 \cos(\omega t) \quad (7)$$

When calculating the impeller for dynamic stability, the determining parameter is the coefficient of dynamism K_d [20,24]:

$$K_d = 1 + \frac{F_u}{p} \cdot \beta \tag{8}$$

where F_i – the centrifugal force of inertia, P – the weight of the rotor; β – the coefficient of oscillation increase.

The coefficient of oscillation increase is determined by the formula [19,20,25]:

$$\beta = \frac{1}{1 - \left(\frac{\omega}{\omega_0}\right)^2} \tag{9}$$

where ω , ω_0 – the frequency of forced and natural vibrations of the impeller.

The dynamicity coefficient characterizes not only the ratio of amplitudes during dynamic and static deformation of an elastic bond, but also the ratio of the corresponding maximum forces and stresses. It follows from the expression for β that the value of the dynamicity coefficient is determined only by the ratio of frequencies ω/ω_0 . The curve of the corresponding dependence is called the amplitude-frequency response (Fig. 7).

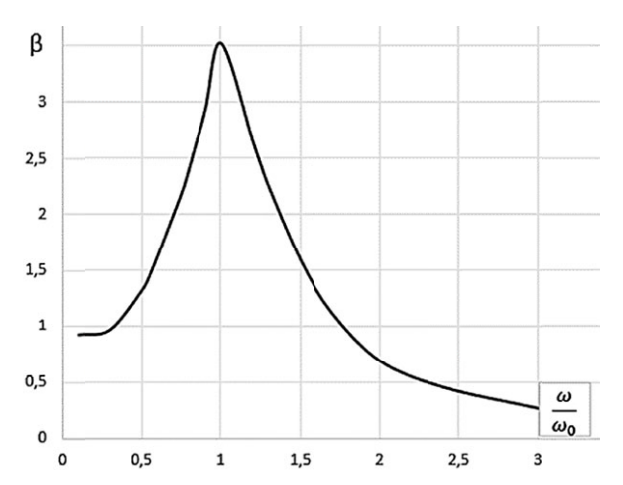


Fig. 7. Amplitude-frequency response of the pump

At $\omega < \omega_0$, the oscillations of the system occur in the same phase with the driving force, and the amplitude of the oscillations is close to the deformation of the elastic bond under its static loading by force $F(\beta \approx 1)$.

At $\omega > \omega_0$ coefficient $\beta < 0$, the oscillation of the system occurs in antiphase with a driving force F, and in the limit at $\omega \to \infty$ amplitude $x \to 0$. The effect of reducing dynamic deformation and stress is explained by the fact that the low-frequency elastic system »does not have time« to respond to rapid changes in the disturbing force.

The most dangerous case is resonance, when the angular velocity of rotation of the rotor ω coincides with the frequency of natural oscillations of the system ω_0 . That is, when $\omega=\omega_0$ (Fig. 14). When the frequencies of the forced and natural oscillations of the system are equal, the amplitude of the forced oscillations tends to infinity $(\beta \to \infty)$. This phenomenon forms a resonant state, and the corresponding frequency of forced oscillations is converted into a resonant one.

If the frequency ω of forced oscillations is set, for example, by the conditions of the technological process, then the frequency of natural oscillations of the system is changed in one way or another. Optimal conditions for the long-term functioning of the system when the ratio ω/ω_0 was greater than one, since in such a case it is possible to obtain a dynamism coefficient $\beta < 1$.

The natural oscillation frequency (ω_0) is determined by the magnitude of the oscillating mass and the rigidity of the system:

$$\omega_{0i} = f(i) \cdot C \sqrt{\frac{E}{12\rho(1-\mu^2)}} \quad \text{or } \omega_{0i} = f(i) \cdot C \cdot K \quad (10)$$

where f(i) – a coefficient depending on the natural frequency of the structural element; C – a coefficient depending on geometry and boundary conditions; E – the modulus of elasticity; p – the density of the material; μ – the Poisson's ratio; K – a coefficient depending on the modulus of elasticity of the material (E), the density of the material (p) and the Poisson's ratio (μ) .

As can be seen, the values of the natural frequencies of the structural element will depend on the physical and mechanical characteristics of the materials and geometric dimensions.

This means that the condition of vibration resistance according to the criterion of natural frequencies is expressed as: the natural frequencies of the structure must lie outside the frequency range of external influences, namely:

$$f_i \notin [0.7 f_{\min}^{impact}, 1.3 f_{\max}^{impact}]$$
 (11)

where fi - i-th is the natural frequency of the structure; f_{\min}^{impact} , f_{\max}^{impact} – the lower and upper frequency of the range of external vibration effects.

According to the recommendations of J.F. Gulich, in order to ensure vibration-reliable operation of the rotor, the nominal rotation frequency of its shaft n should differ from the critical by 25...30% up or down.

Resonances at lower natural frequencies ($i \le 5$) are usually the most dangerous, since they accumulate most of the mechanical energy.

3. Modal analysis of vibration frequencies of five vibration forms

Frequency analysis in APM FEM makes it possible to estimate the natural frequency spectrum of the structure at the preliminary design stage. Further, it is possible to optimize the design parameters of the product in order to achieve a con-

dition of frequency vibration resistance. To increase the natural frequencies, it is necessary to give the structure more rigidity and (or) reduce its mass. The calculation of the frequencies and forms of natural vibrations of the impeller was carried out for a rotation speed of n = 1,500 rpm. The boundary conditions are rotation around the axis of the wheel hub and the absence of movement of the impeller base along this axis.

A modal analysis was performed to determine the natural shapes and frequencies of vibrations. Sixteen shapes and frequencies of blade vibrations are calculated, falling in the range from 100 to 6,000 Hz. The results are presented in TABLE 6. The first five forms of natural vibrations are shown in Fig. 8. For a complex geometric body – the blades – the first shape is the first torsional shape of the blade vibrations. The second shape is the first bending shape. The third is the second bending, the fourth and fifth are complex bending and torsional shapes.

The results of the frequency analysis are the calculated natural frequencies of the product and their corresponding natural waveforms. The waveforms represent the relative amplitudes of the displacements of the structure in the nodes of the finite element grid. According to them, it is possible to determine the nature of the movement carried out by the system at an oscillation frequency corresponding to its own [24,25].

The shape of the vibrations shows what relative deformations (displacements) the structure experiences in the event of resonance at the corresponding natural frequency (Fig. 9). The waveforms displayed in the program window after the calculation is completed represent the relative amplitudes of the oscillations. Analyzing these shapes, one can conclude about the nature of the resonant displacements, but not about their actual amplitude. Knowing the expected shape of vibrations at a certain natural frequency, it is possible, for example, to set an additional fastening or support in the area of the structure corresponding to the maximum of this shape of vibrations, which will lead to an effective change in the spectral properties of the product.

The results of 3D modeling of the effect of vibration frequencies on the pump impeller made it possible to determine the most dangerous vibration range, which is at a pressure created by a centrifugal pump of 1.5 MPa for Steel 20Cr13C, the natural oscillation frequency is up to $\omega_0 = 106.6 \div 2,325.7$ Hz. As can be

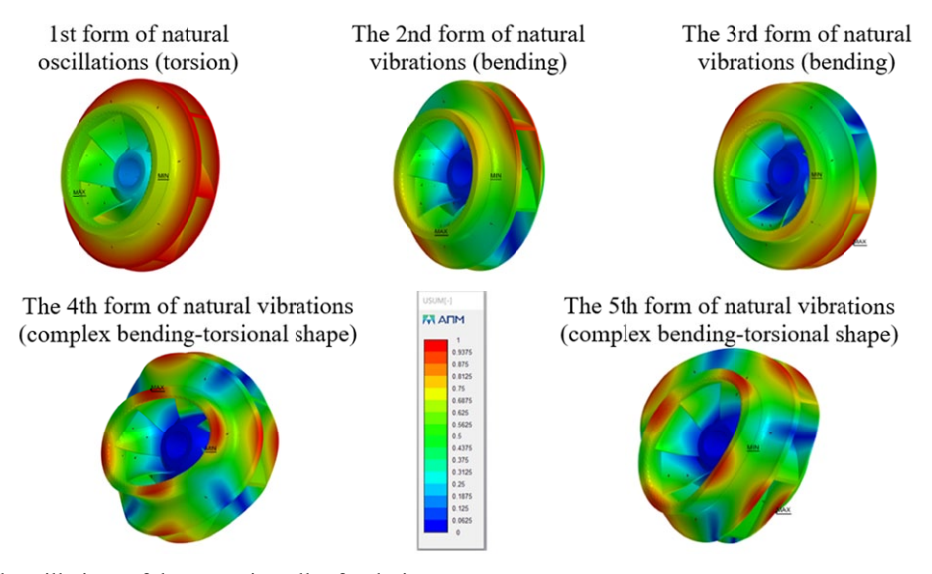


Fig. 8. Forms of natural oscillations of the pump impeller for design pressure

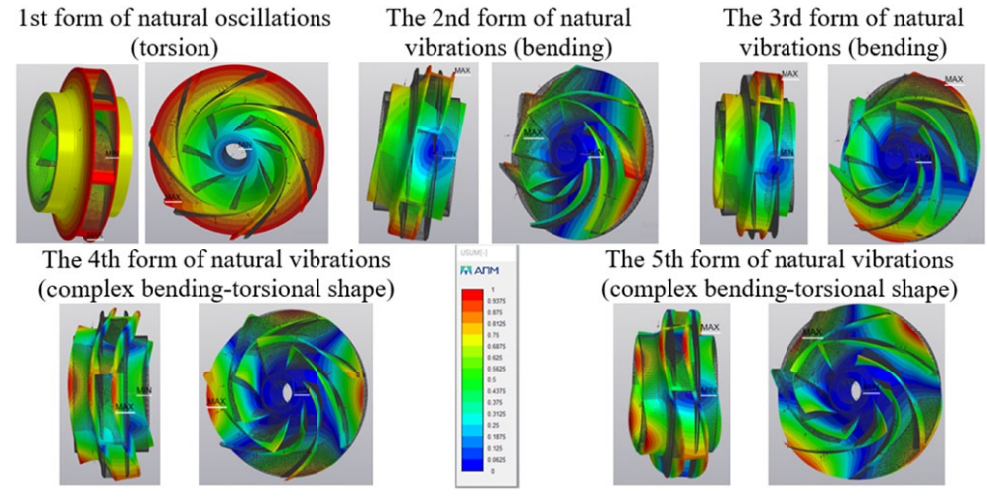


Fig. 9. Simulation of various natural frequencies of the impeller at a frequency of 1,500 rpm

TABLE 6
Calculation results of the natural frequencies of the pump impeller

Design	The results of the calculation of natural frequencies							cies	
pressure,	, Impeller material								
MPa	a Steel 20Cr13C Steel 12Cr7					Cr7Mn3S	·7Mn3SiC		
	N	Частога [рад/ сек]	Частота [Гц]	Период [c]		N	Частота [рад/ сек]	Частэта [Гц]	Период [c]
	1	669.968425	106.628787	0.009378		1	692.951484	110.286654	0.009067
1.5	2	8532.183443	1357.93917	0.000736		2	8238.033241	1311.123712	0.000763
1.5	3	8541.436953	1359.411912	0.000736		3	8247.32461	1312.502479	0.000762
	4	14599.257356	2323.543974	0.00043		4	14101.559374	2244.33288	0.000446
	5	14612.800496	2325.699431	0.00043		5	14117.336726	2246.843923	0.000445
	Ξ	•	•		+		•	•	
	N	Частета [рад/ сек]	Частота [Гц]	Период [с]		N	Частота [рад/ сек]	Частота [Гц]	Период [c]
	1	639.878111	101.839764	0.009819		1	623.14816	99.17711	0.010083
2.5	2	8527.774154	1357.23741	0.000737		2	8242.066829	1311.765677	0.000762
2.3	3	8542.548356	1359.588797	0.000736		3	8257.880874	1314.282561	0.000761
	4	14603.365428	2324.197794	0.00043		4	14091.615546	2242.75027	0.000446
	5	14609.311419	2325.144127	0.00043	1	5	14109.046453	2245.524485	0.000445
	_	•	•		4		-	•	
	N	Частота [рад/ сек]	Частота [Гц]	Период [c]		N	Частота [рад/ сек]	Частота [Гц]	Период [c]
	1	605.677836	96.396622	0.010374		1	689.940618	109.80746	0.009107
4.0	2	8534.94776	1358.379125	0.000736		2	8232.747983	1310282537	0.000763
7.0	3	8546.475694	1360.213853	0.000735	1	3	8248.969082	1312.864205	0.000762
	4	14587.505559	2321.673617	0.000431		4	14100.275893	2244.128607	0.000446
	5	14605.742337	2324.576091	0.00043		5	14117.858236	2246926924	0.000445

seen from TABLE 6, the sample is taken for 5 main periods, since with a further increase in the speed of rotation of the impeller, the vibration range becomes constant without significant fluctuations. This dependence is confirmed by the characteristics of the other material Steel 12Cr7Mn3SiC under the same pressure conditions of 1.5 MPa, the critical frequency of natural oscillations reaches $\omega_0 = 2,247$ Hz. The five forms of natural vibrations (Fig. 9) clearly demonstrate the zones of location of the maximum values of vibration loading, which fall on the extreme part of the wheel diameter with the maximum effect of dynamic forces. This distribution of the vibrational dynamic load explains the constant types of defect – fragments of the pump impeller in the same cross-sectional plane of the wheel made of different materials Steel 20Cr13C and Steel 12Cr7Mn3SiC (Fig. 10).

It has been established that both disc breakage and corrosion-erosive wear occur in the same area of exposure to maxi-





Fig. 10. Wheel defects: a - wheel disc breakage; b - corrosion wear

mum dynamic and centrifugal loads – the upper part of the wheel diameter. And an increase in the natural frequency of vibrations to ω_0 = 2,247 Hz, with a yield strength of 1,079 [N/mm²], low-frequency destruction of the interatomic bonds of the 20Cr13C material occurs in a corrosive environment.

As a confirmation of the hypothesis that the service life and the forecast period of uptime of the pump is more accurate (more than 17%) when studying changes in the phase structure of the material under the influence of vibrational vibration frequencies that form the stress concentration in the metal at the stage of microcrack nucleation.

It was found that the natural rotational speeds of the impeller (>100 Hz) are 75% higher than the operating rotational speed of the structure (25 Hz), which indicates sufficient rigidity of the wheel structure for the selected materials. At the same time, the choice of material has a negligible effect (within 10%) on the results obtained. Thus, at low speeds and low pressure, additional measures are not required to ensure the reliability of the wheel from the effects of vibration loads. However, the nature of the forms of natural vibrations clearly shows the sections of the structure most susceptible to destruction, which, together with the static calculation data, makes it possible to make the necessary improvements.

4. The results of experimental studies of the effect of high-frequency vibrations on the phase structure of the material

During metallographic studies, the damaged part of the sample, exposed to maximum loads, was cut out and pressed into acrylic resin, followed by grinding and polishing. The optical metallographic study was performed on an inverted Eclipse MA200 microscope (Nikon, Japan) at a magnification of 500×. Microhardness was measured using an automatic HMV-GRAD microhardness meter (Shimadzu, Japan) in accordance with GOST 9450-76.

TABLE 7 shows the results of high-frequency tests of pump impeller samples made of 20Cr13C steel with identified defects. Since the yield strength of this steel is at the level of 450 MPa, stress amplitudes close to this value – 300 MPa and 450 MPa were selected for two samples. For the third sample, an amplitude of 500 MPa was selected to assess the effect of high-frequency loads exceeding the static yield strength of this steel.

TABLE 7
The results of high-frequency tests of samples of the impeller of the pump made of 20Cr13C steel with identified defects

No.	Voltage amplitude σ _a , MPa	Number of cycles, N	Visible changes
1	300	$1.3465 \cdot 10^8$	Uniformity of the phase of the structure
2	450	5.4489·10 ⁸	Uniformity of the phase of the structure
3	500	$9.7875 \cdot 10^5$	Crack

Fig. 11, a shows the structure of the recovered part of sample 1. This part has a more dispersed structure than the base metal. The characteristic size of ferritic grains in the welding zone is 5-20 μ m. Fig. 11b shows the structure of the central (most loaded) part of sample 1, and Fig. 11c shows the structure near the base of the wheel of the first sample. Fig. 11b shows that the structures of the lower base of the pump wheel and the central part are almost identical. The characteristic grain size of ferrite is 10-20 μ m.

Thus, there are no visible signs of fracture or plastic deformation in the central (most loaded) part of this sample.

Test sample No. 2 (Fig. 12a,b).

The structure at the base of the wheel (Fig. 12a) is typical for 20Cr13C steel. The characteristic size of ferritic grains is about 20 μ m. Grain grinding is noticeable in the central part of the sample (Figure 12,b). The characteristic size of ferrite grains in this zone is 5 – 10 μ m. Otherwise, there are no differences from the structure of the impeller base, and there are no signs of destruction either.

Fig. 13a, b shows the structure of the third sample in the following study areas: at the base of the impeller, at a distance of 3 mm from the crack (the boundary of the change in the phase grains of the pre-fracture) in the center and near the crack itself.

At the base of the impeller of the centrifugal pump (Fig. 13a), the sample has a structure typical of low-carbon steel of the pearlite class. The characteristic size of ferritic grains is $20~\mu m$. Minimal loads are applied on the basis of the impeller of the sample, so its structure corresponds to the original one.

At a distance of 3 mm from the crack (Fig. 13b), a transition to a more dispersed structure is noticeable: as you approach

the crack, the characteristic size of ferritic grains decreases to $5\text{--}10\,\mu\text{m}$ (Fig. 13c). Thus, cyclic loads of vibrational frequencies led to grain crushing and the appearance of a crack in the most loaded part of the sample 3.

The average microhardness values for the zones of sample 1 are shown in TABLE 8. For the welding zone, only the microhardness values of ferrite are indicated: the perlite content in the deposited metal is small, and it is difficult to measure its microhardness.

Microhardness of sample No. 1

TABLE 8

The area of the test sample	Ferrite, HV	Perlite, HV	
Recovery area	228-285	_	
The base of the pump impeller	195-219	212-244	
The central part	193-217	193-242	

The recovered metal section of the impeller in the zone of thermal influence has an increased microhardness (\sim 270-280 HV for ferrite). Presumably, high microhardness is achieved by the presence of alloying elements in ferrite – manganese and silicon. At the same time, the hardness values at the base of the impeller and in the central part are almost the same – about 200-210 HV for ferrite and \sim 220-230 HV for perlite.

The microhardness data of sample 2 are shown in TABLE 9. The average hardness values of the main part of the wheel are 173 HV for ferrite and 188 HV for perlite, in the central part – respectively 193 HV for ferrite and 212 HV for perlite. Thus, the microhardness of the central part of sample 2 is 20-25 HV higher than the base of the wheel.

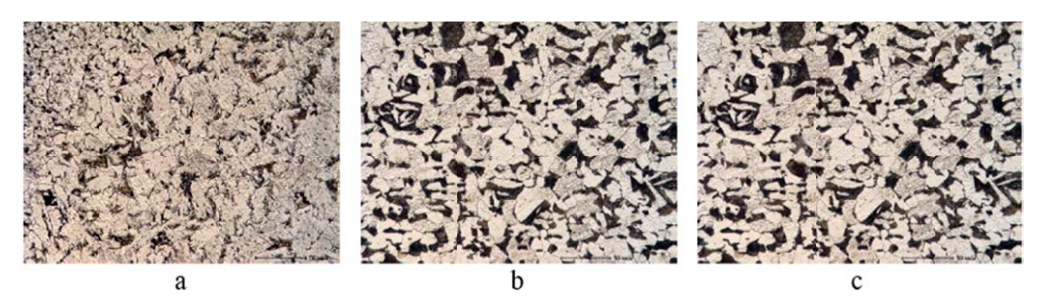


Fig. 11. Microstructure of sample No. 1 after testing at an increase of 500×: a - recovery zone; b - central part; c - base of the impeller

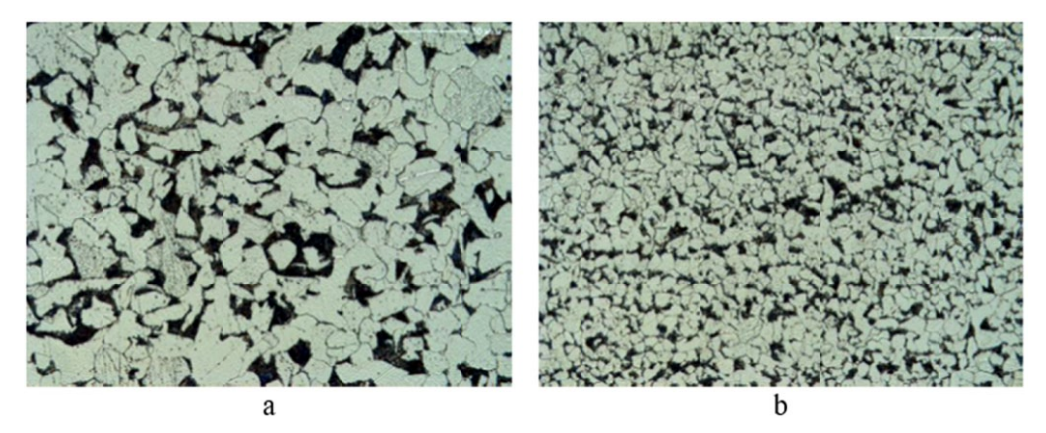


Fig. 12. The microstructure of sample No. 2 after testing at an increase of 500×: a – the base of the impeller; b – the central part

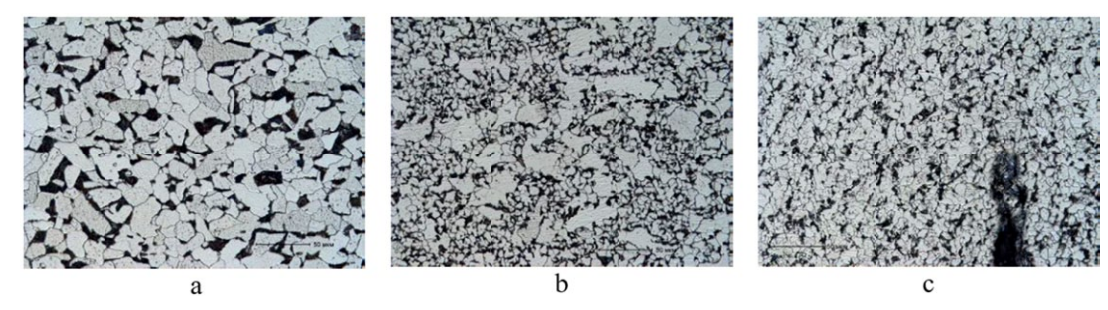


Fig. 13. Microstructure of sample No. 3 after testing at an increase of $500\times$: a – the base of the impeller; b – 3 mm from the crack; c – the tip of the crack

TABLE 9 Microhardness of sample No. 2

The area of the test sample	Ferrite, HV	Perlite, HV
The base of the pump impeller	160-184	169-202
The central part	189-200	185-241

Data on the microhardness of sample No. 3 are given in TABLE 10. Studies have found that at the base of the pump impeller and at a distance of 3 mm from the crack, the hardness has values characteristic of 20Cr13C steel (\sim 180 HV for ferrite and 200-210 HV for perlite), and only in the immediate vicinity of the crack, at a distance of less than 100 μ m, the hardness increases (\sim 240 HV for ferrite and \sim 260 HV for perlite).

TABLE 10 Microhardness of sample No. 3

The area of the test sample	Ferrite, HV	Perlite, HV
The base of the pump impeller	157-195	195-229
At a distance of 3 mm from the crack	135-207	171-218
Crack detection area	213-278	198-308

5. Conclusions

According to the results of the research, the following conclusions are drawn:

- 1. It was found that the natural frequencies of the impeller (>100 Hz) are 75% higher than the operating speed of the structure (25 Hz), which indicates sufficient rigidity of the wheel structure for the selected materials. At the same time, the choice of material has a negligible effect (within 10%) on the results obtained. Thus, at low speeds and low pressure, additional measures are not required to ensure the reliability of the wheel from the effects of vibration loads. However, the nature of the forms of natural vibrations clearly shows the areas of the structure that are most susceptible to destruction, which, together with the data of the static calculation, makes it possible to make the necessary improvements.
- 2. To calculate the structure, taking into account the structural and technological elements (holes, fasteners, chamfers, rounding), a powerful calculation station is needed. An

attempt was made to calculate the complete design on a workstation equipped with two processors of 24 cores each, 256 GB of RAM and two Tesla graphics cards. The time for generating the finite element grid and calculating the design parameters in APM FEM was interrupted after 15 hours due to an internal program error. It is necessary to optimize the constructed model and the parameters of the finite element grid construction. This approach is too labor-intensive to perform multiple preliminary calculations, so a simplified impeller model was used.

- 3. Currently, there is no available data on the effect of cyclically varying loads on changes in the structural components of the material (grain size, phase composition fine-grained martensite) during long-term operation of the pump. In order to obtain the necessary set of properties to ensure the calculated operational parameters of machine parts and assemblies, it is necessary to select the structure and composition of the material, as well as the manufacturing technology of the part.
 - The characteristics of the elastic properties of the material are Young's modulus (E), Poisson's ratio (μ) , shear modulus (G) and volumetric modulus of elasticity (K). All these parameters are interconnected and depend on the energy of interatomic bonds and on the interatomic distance.
- 4. Based on an experimental metallographic study and measurement of the microhardness of 20Cr13C steel samples, it was found that fatigue changes in the phase structure of 20Cr13C steel at high frequency loads led to grain grinding. Fatigue changes in the structure of 20Cr13C steel lead to an increase in the microhardness of the sample. Thus, microhardness measurement can be applied in parallel with metallography as one of the criteria for the vibration resistance of a material for more reliable detection of changes.
- 5. Sample 1 worked 1.35·10⁸ cycles at an amplitude of 300 MPa. Neither metallography nor microhardness showed any changes in it. Thus, the restored 20Cr13C steel parts based on 10⁸ cycles can withstand cyclic loads with an amplitude of up to 300 MPa.
- 6. Sample 2 has worked 5.45·10⁸ cycles at an amplitude of 450 MPa, after which changes in its structure and microhardness are observed. This means that for 20Cr13C steel based on 10⁸ cycles, the voltage amplitude of 300 MPa is not safe.

7. Vibration with a frequency of 20 kHz and a loading amplitude of 500 MPa leads to grinding of the 20Cr13C steel structure and the appearance of fatigue cracks.

Funding

BR18574035 program »Development, development, application of scientific and technological methods and digital tools to increase the productivity and competitiveness of pumping industry in Kazakhstan at the level of Industry 4.0«.

REFERENCES

- [1] T. Nguyen Ngoc, V.M. Kapralov, Analysis of resonance and natural frequencies of gas turbine blades. St. Petersburg Polytechnic University Journal of Engineering Science and Technology 25 (2), 149-160 (2019). DOI: https://doi.org/10.18721/JEST.25212
- [2] A.I. Shvindin, Vibration reliability. Neftegaz. RU 4, 90-93 (2016). https://magazine.neftegaz.ru/articles/tekhnologii/628102-vibratsionnaya-nadezhnost/, accessed: 17.04.2022
- [3] V.V. Savinkin, S.N. Kolisnichenko, A.V. Sandu, O.V. Ivanova, P. Vizureanu, Z.Z. Zhumekenova, Investigation of the strength parameters of drilling pumps during the formation of contact stresses in gears. Appl. Sci. 11, 7076-1-7076-22 (2021). DOI: https://doi.org/10.3390/app11157076
- [4] V.V. Savinkin, Z.Zh. Zhumekenova, O.V. Ivanova, A.V. Sandu, S.N. Kolisnichenko, Study of wear and redistribution dynamic forces of wheel pairs restored by a wear-resistant coating 15Cr-17Ni12V3F. Coatings 11 (12), 1441 (2021). DOI: https://doi.org/10.3390/ coatings11121441
- [5] M.M. Zakirnichnaya, T.Ph. Khalitov, Detection of cracks in centrifugal pump shaft on stream using high-frequency components of vibration spectrum. The oil business. Oil refining machines and apparatuses 9 (1), 53-59 (2011).
- [6] O.A. Volokhovskaya, On one approach to reducing the vibration level of submersible centrifugal pumps for oil production. Bulletin of the Nizhny Novgorod University named after N.I. Lobachevsky 4 (2), 82-84 (2011).
- [7] http://vibropoint.ru/vibrodiagnostika-nasosov/, accessed: 20.09.2023
- [8] S. Madhavan, Ja. Rajeev, C. Sujatha, A.S. Sekhar, Vibration based damage detection of rotor blades in a gas turbine engine. Engineering Failure Analysis 46, 26-39 (2014). DOI: https://doi.org/10.1016/f.engfailanal.2014.07.021
- [9] D.N. Popov, N.T. Sosnovskiy, M.V. Siukhin, Hydrodynamic loading of centrifugal pumps rotors during transient processes. Science and Education. Mechanical Engineering and Computer Technology 12, 1-9 (2011).
- [10] Jafari Pedram, Reduction of vibration of hydrodynamic origin of pumping and power units. Scientific Bulletin of the Moscow State Technical University of Civil Aviation 173, 137-140 (2011).
- [11] V.N. Kyznetsova, V.V. Savinkin, T.Yu. Ratushnaya, A.V. Sandu, P. Vizureanu, Study of the spatial distribution of forces and

- stresses on wear surfaces at optimization of the excavating part of an earthmoving machine transverse profile. Coatings 11 (2), 182 (2021). DOI: https://doi.org/10.3390/coatings11020182
- [12] V.V. Savinkin, P. Vizureanu, A.V. Sandu, A.A. Ivanischev, A. Surleva, Improvement of the turbine blade surface phase structure recovered by plasma spraying. Coatings 10 (1), 62 (2020).
 DOI: https://doi.org/10.3390/coatings10010062
- [13] N.V. Kutsubina, A.A. Sannikov, Theory of vibration protection and acoustic dynamics of machines: textbook, Ural State Forestry University, Yekaterinburg (2014).
- [14] A.R. Denisova, O.L. Nikolaeva, Investigation of the oscillatory vibration process of rotary mechanisms. Proceedings of the XIV All-Russian Open Youth Scientific and Practical Conference. Kazan State Energy University, 64-68 (2019). https://elibrary.ru/item.asp?id = 44136724
- [15] V.N. Ivanovsky, A.A. Sabirov, A.V. Degovtsov, S.S. Pekin, Yu.A. Donskoy, S.V. Krivenkov, N.N. Sokolov, A.V. Kuzmin, Design and research of characteristics of degrees of dynamic pumps: educational publication. Gubkin Russian State University of Oil and Gas, Moscow (2014).
- [16] J.F. Gulich (Ed.), Centrifugal Pumps, Springer, Berlin Heidelberg (2010). DOI: https://doi.org/10.1007/978-3-642-12824-0
- [17] M.N. Grebennikov, N.I. Pekelny, Theories of strength: complex resistance, National Aerospace University named after N.E. Zhukovsky «Kharkiv Aviation Institute», Kharkov (2016).
- [18] A.V. Grigoriev, Assessment of vibration intensity based on the analysis of the image of a round-shaped test object with vibration blur. News of universities. The Volga Region. Technical Sciences 3 (63), 5-14 (2022). DOI: https://doi.org/10.21685/2072-3059-2022-3-1
- [19] https://emk24.ru/about/, accessed: 17.05.2023
- [20] M.A. Vikulov, N.P. Ovchinnikov, Dynamic calculation of the pump rotor. Mining Information and Analytical Bulletin (Scientific and Technical Journal) **9**, 359-364 (2014).
- [21] I.A. Birger, Strength, stability, vibrations: Handbook 1, Mashinostroenie, Moscow (1968)
- [22] D.S. Vakhlyarsky, A.M. Guskov, Numerical analysis of the dynamics of the rotor of a centrifugal pump. Bulletin of the Bauman Moscow State Technical University. Mechanical Engineering Series 6 (6), 34-49 (2012).
- [23] V.V. Savinkin, T.Yu. Ratushnaya, A.A. Ivanischev, A.R. Surleva, O.V. Ivanova, S.N. Kolisnichenko, Study on the optimal phase structure of recovered steam turbine blades using different technological spray modes for deposition of Al₂O₃. IConGDM and IConGEET, 64 (2019).
- [24] V.V. Savinkin, V.N. Kuznetsova, T.Yu. Ratushnaya, L.A. Kiselev, Method of integrated assessment of fatigue stresses in the structure of the restored blades of CHP and HPS. Bulletinof the Tomsk Polytechnic University. Geo Assets Engineering 330 (8), 65-77 (2019). DOI: https://doi.org/10.18799/24131830/2019/8/2213
- [25] V.N. Kuznetsova, V.V. Savinkin, More efficient rotation of excavator platforms. Russ. Engin. Res. 37 (8), 667-671 (2017).
 DOI: https://doi.org/10.3103/S1068798x1708010x